

AD/

ESD-TR-85-317

Annual Report

Low-RF-Loss Superconductive Thin-Film Alloys

31 May 1985

Lincoln Laboratory
MASSACHUSETTS INSTITUTE OF TECHNOLOGY
LEXINGTON, MASSACHUSETTS



Prepared for the Department of the Navy
under Electronic Systems Division Contract F19628-85-C-0002.

Approved for public release; distribution unlimited.

ADA166876

The work reported in this document was performed at Lincoln Laboratory, a center for research operated by Massachusetts Institute of Technology. This work was sponsored by the Department of the Navy under Air Force Contract F19628-85-C-0002.

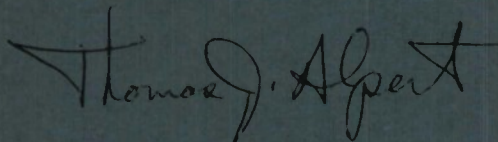
This report may be reproduced to satisfy needs of U.S. Government agencies.

The views and conclusions contained in this document are those of the contractor and should not be interpreted as necessarily representing the official policies, either expressed or implied, of the United States Government.

The ESD Public Affairs Office has reviewed this report, and it is releasable to the National Technical Information Service, where it will be available to the general public, including foreign nationals.

This technical report has been reviewed and is approved for publication.

FOR THE COMMANDER

A handwritten signature in dark ink, reading "Thomas J. Alpert". The signature is fluid and cursive, with the first name "Thomas" and last name "Alpert" clearly legible.

Thomas J. Alpert, Major, USAF
Chief, ESD Lincoln Laboratory Project Office

Non-Lincoln Recipients

PLEASE DO NOT RETURN

Permission is given to destroy this document
when it is no longer needed.

MASSACHUSETTS INSTITUTE OF TECHNOLOGY
LINCOLN LABORATORY

**LOW-RF-LOSS SUPERCONDUCTIVE
THIN-FILM ALLOYS**

ANNUAL REPORT
TO THE
OFFICE OF NAVAL RESEARCH

R.W. RALSTON

Group 86

1 JUNE 1984 — 31 MAY 1985

ISSUED 18 MARCH 1986

Approved for public release; distribution unlimited.

LEXINGTON

MASSACHUSETTS

ABSTRACT

→ Stripline resonators in conjunction with an automated RF setup were used to determine RF losses in films of Nb, NbN and Nb₃Sn. Variation in the losses with frequency for some of these films seems to be associated with particulate contamination during deposition. However, measurements also indicate that if clean films can be deposited they could be used for very long delay lines (hundreds of nanoseconds) at temperatures compatible with existing closed-cycle cryocoolers.

High RF losses in Nb films deposited by ion beam sputtering have been shown to be associated with contamination from stainless steel sputtered from fixtures in the chamber. Nb shadow masks were used to collimate the beam and this eliminated the problem. Reactively sputtered films of NbN deposited in this system onto heated substrates have transition temperatures as high as 14 K.

A series of thick film pastes selected for their good insulating properties were used to form insulating layers on NbN. Two of these pastes adhered well to the NbN. Interaction with the NbN seems to be confined to a layer of 100 Å.

→ Keywords: Nb shadow masks,
Niobium, Niobium-tin,
Nitride

Accession For	
NTIS CRA&I	<input checked="" type="checkbox"/>
DTIC TAB	<input type="checkbox"/>
Unannounced	<input type="checkbox"/>
Justification	
By	
Distribution /	
Availability Codes	
Dist	Avail and/or Special
A-1	



TABLE OF CONTENTS

	<u>Page</u>
ABSTRACT.....	iii
1. Characterization of RF Losses of Superconductive Films.....	1
2. RF Measurement Results.....	4
2.1 Nb Films.....	4
2.2 NbN Films.....	4
2.3 Nb ₃ Sn Films.....	8
2.4 Discussion.....	8
3. Ion Beam Deposition of Nb and NbN Thin Films.....	11
3.1 Nb Films.....	11
3.2 NbN Films.....	13
3.3 Discussion.....	16
3.4 The New Ion Beam System.....	18
4. Insulators.....	19
5. Further Work.....	21
APPENDIX A.....	23
REFERENCES.....	26

1. Characterization of RF Losses of Superconductive Films

We have developed a technique using resonators¹ to measure the RF losses of niobium films deposited in our laboratory. As part of this contract we have extended this work to evaluate the RF losses of a series of materials deposited in our laboratory, and elsewhere, as both a function of temperature (between 4.2 K and 25 K) and frequency (200 MHz to 18 GHz). The basic structure is shown schematically in Fig. 1. The resonator is formed by a section of a stripline transmission line weakly coupled by gap capacitors to the measuring circuitry. At frequencies f_n , for which the section of line between the capacitors is an integral number of half wavelengths long, we will observe a resonant peak in transmission whose width and height depend on the losses of the line.

The size of the sample used was dictated in part by the variable temperature dewar used (JANIS Vari-Temp). The substrates are 1/2 in. x 1 in. long. They are, typically, 20 mil thick Tyco sapphire (c-axis parallel to the plane of the deposited film) or 5 mil thick Crystal System sapphire (c-axis perpendicular to the plane). Typically, three films are necessary. Most deposition systems require clamping the substrate to a heater block, thus precluding the deposition of films on both sides of the substrate. A typical package configuration is shown in Fig. 2. Careful grounding is essential, otherwise the feedthrough from the input line to the output line can bypass the weakly coupled resonator and obscure the resonance peaks. The whole structure is kept together by a bed of springs. This is necessary to avoid relative movement of the three films which can result in microphonics that can shift the resonant frequency.

The measurements are made using either a manual scalar network analyser consisting of a spectrum analyser with a tracking generator (for $f < 1800$ MHz)

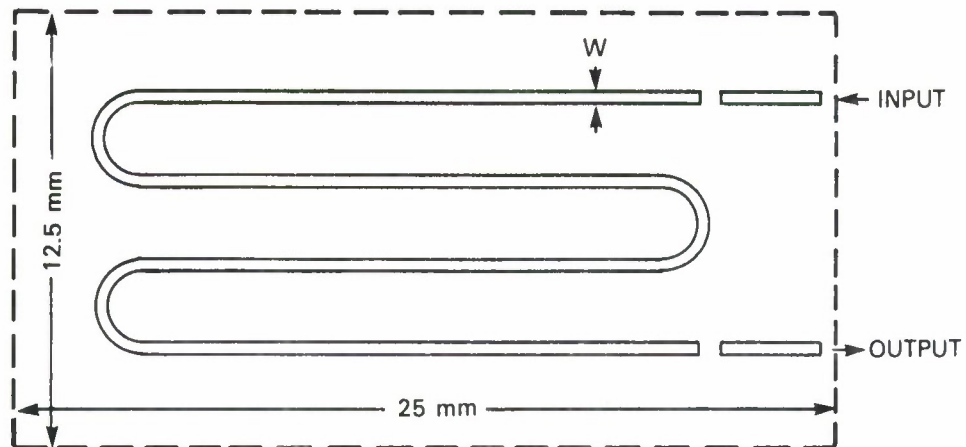


Figure 1. Photolithographic pattern of a thin-film superconductive strip-line resonator.

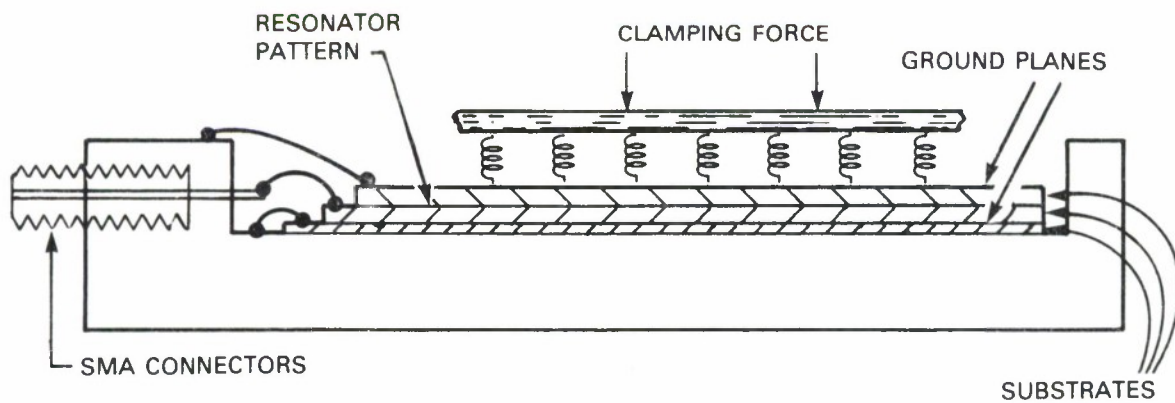


Figure 2. Superconducting resonator package.

153908-N

153909-N-01

or an automatic vector network analyser (for $2 \text{ GHz} < f < 18 \text{ GHz}$). In the JANIS Vari-Temp dewar the sample is surrounded by a stream of helium gas vaporized from the liquid. The temperature of the gas is controlled by a heater situated at the bottom of the sample chamber. A needle valve connected between the porous heater and the liquid He reservoir controls the amount of helium reaching the heater. This valve is set at the beginning of the experiment. After this, the sample temperature is controlled by the amount of power delivered to the heater. A Lake Shore programmable controller in conjunction with a Si diode thermometer allows for the control of the heater temperature. A second Si diode thermometer is mounted inside the resonator package. A third Ge resistance thermometer also mounted inside the package and traceable to the National Bureau of Standards is used to check the accuracy of the sample temperature. The temperature controller, the resistance thermometer, and the network analyser are interfaced with an HP-85 microcomputer through an IEEE 488 bus. A computer program keeps track of the sample temperature and compensates the heater temperature in order to keep the sample temperature constant. The temperature of the package as measured by the Ge thermometer does not change by more than 50 mK during a typical frequency scan.

The resonant frequencies are found at 4.2 K using a semi-automatic procedure. The frequency scan is automatic but the operator, prior to the scan, manually determines the center frequency for each resonance. This procedure was chosen after a totally automatic procedure proved to be too slow. Once the resonant frequencies are found the program allows for the complete automatic measurement of the Q and insertion losses for frequencies larger than 2 GHz and for temperatures between 4.2 K and the transition temperature of the sample being evaluated. For lower frequencies the manual scalar analyser is used. In

this case, the HP-85 is used to control the temperature and it prompts the operator to enter the data manually obtained from the spectrum analyser screen. Internal checks for incompatibilities of the measured Q are performed by the program in the HP-85 and error messages are displayed if the results are much different from the expected ones. If the resonant peaks are obscured by feedthrough, the automatic network analyzer can be instructed to measure the feedthrough magnitude and phase at several frequencies above and below the resonance. These measurements are interpolated across the resonance and subtracted from the measured data, resulting in a feedthrough suppression of, typically, 20 dB.

A detailed analysis of the resonator structure and how to relate the Q measurements to surface resistance in the films is presented in Appendix A.

2. RF Measurement Results

2.1 Nb Films

Figure 3 illustrates a typical result for a 3000-Å thick film deposited in our facilities by RF diode sputtering. These films typically have a transition temperature (T_C) of 9 K and are polycrystalline.

Figure 4 is the result of a 2500-Å film deposited by evaporation in an ultrahigh vacuum system onto a substrate held at 800°C. This film was furnished by Westinghouse.

2.2 NbN Films

Films deposited at NRL by E. J. Cukauskas and W. L. Carter were evaluated using this same technique. The films were 1.5-μm thick, and were RF reactively sputtered onto 600°C substrates using a magnetron like configuration. The system used was a UHV system backed by a turbo pump. Methane was used during the sputtering (so the films are really NbC_xN_y). The results are shown in Fig. 5.

(LL-I)

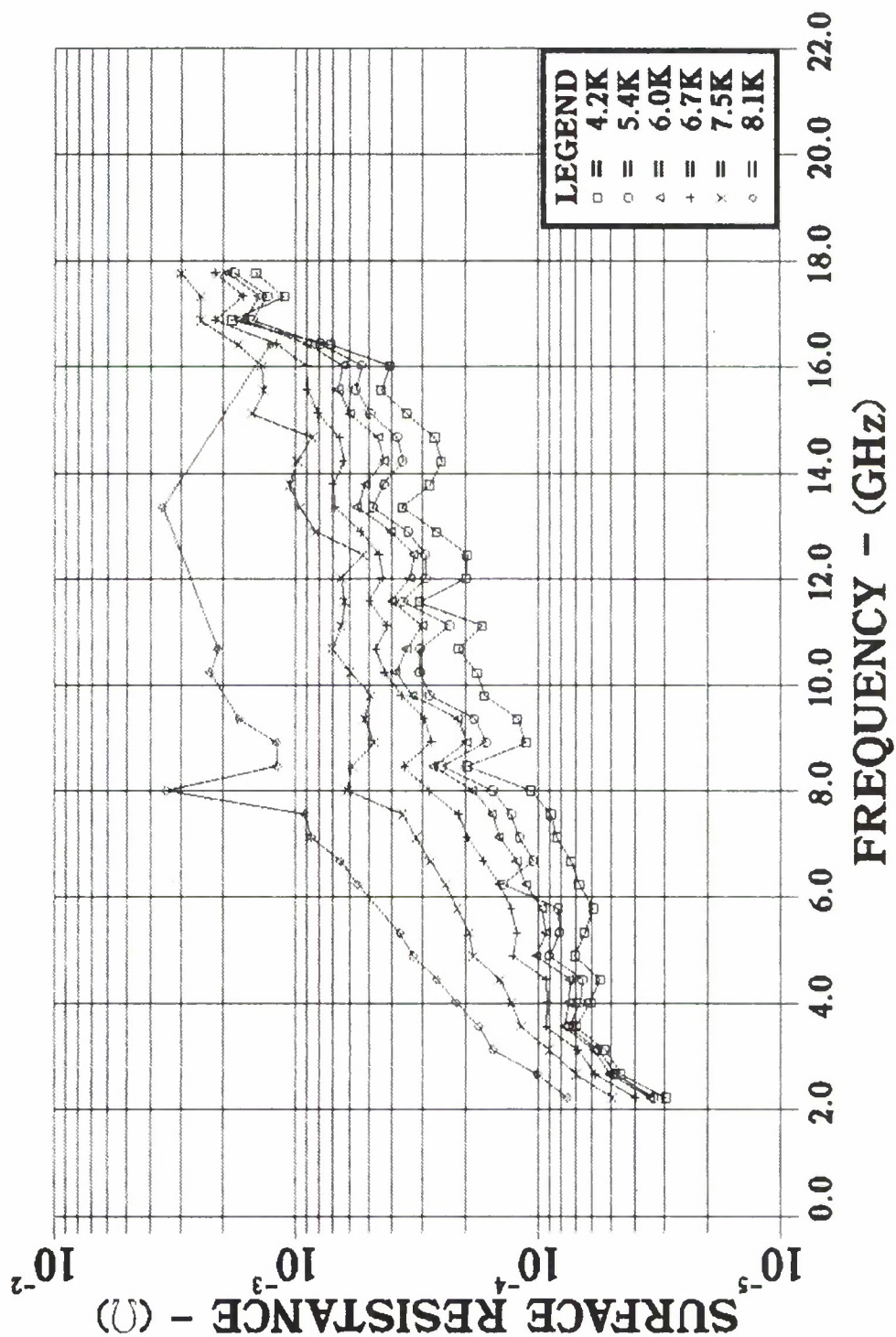


Figure 3. Variation of the surface resistance with frequency for a 3000 Å Nb film sputter-deposited onto a sapphire substrate at Lincoln Laboratory.

(WESTINGHOUSE)

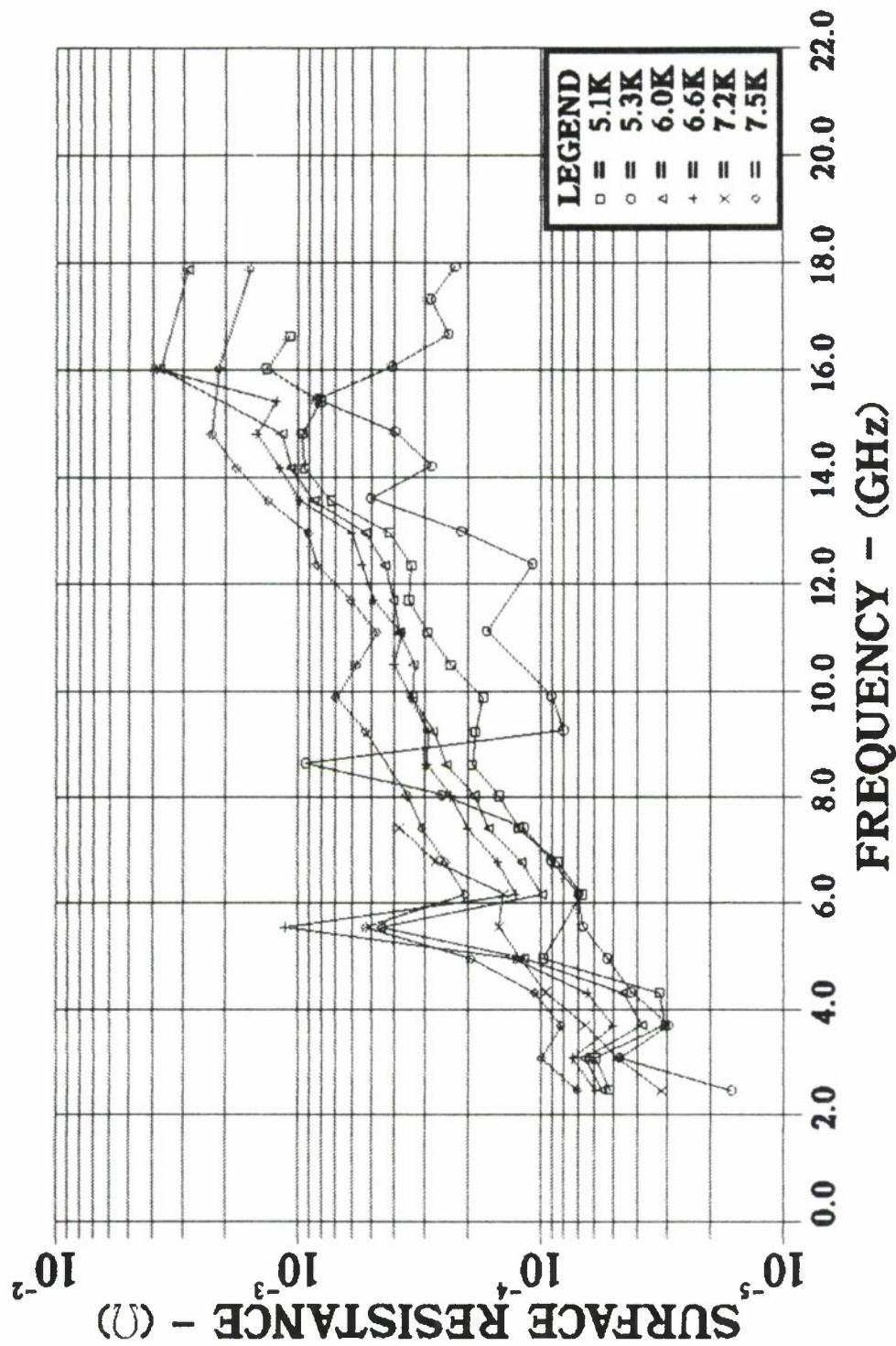


Figure 4. Variation of the surface resistance with frequency for a 2500 Å Nb film deposited on sapphire by E-beam evaporation under ultra-high-vacuum conditions. (Westinghouse Research Center)

NbN - (NRL)

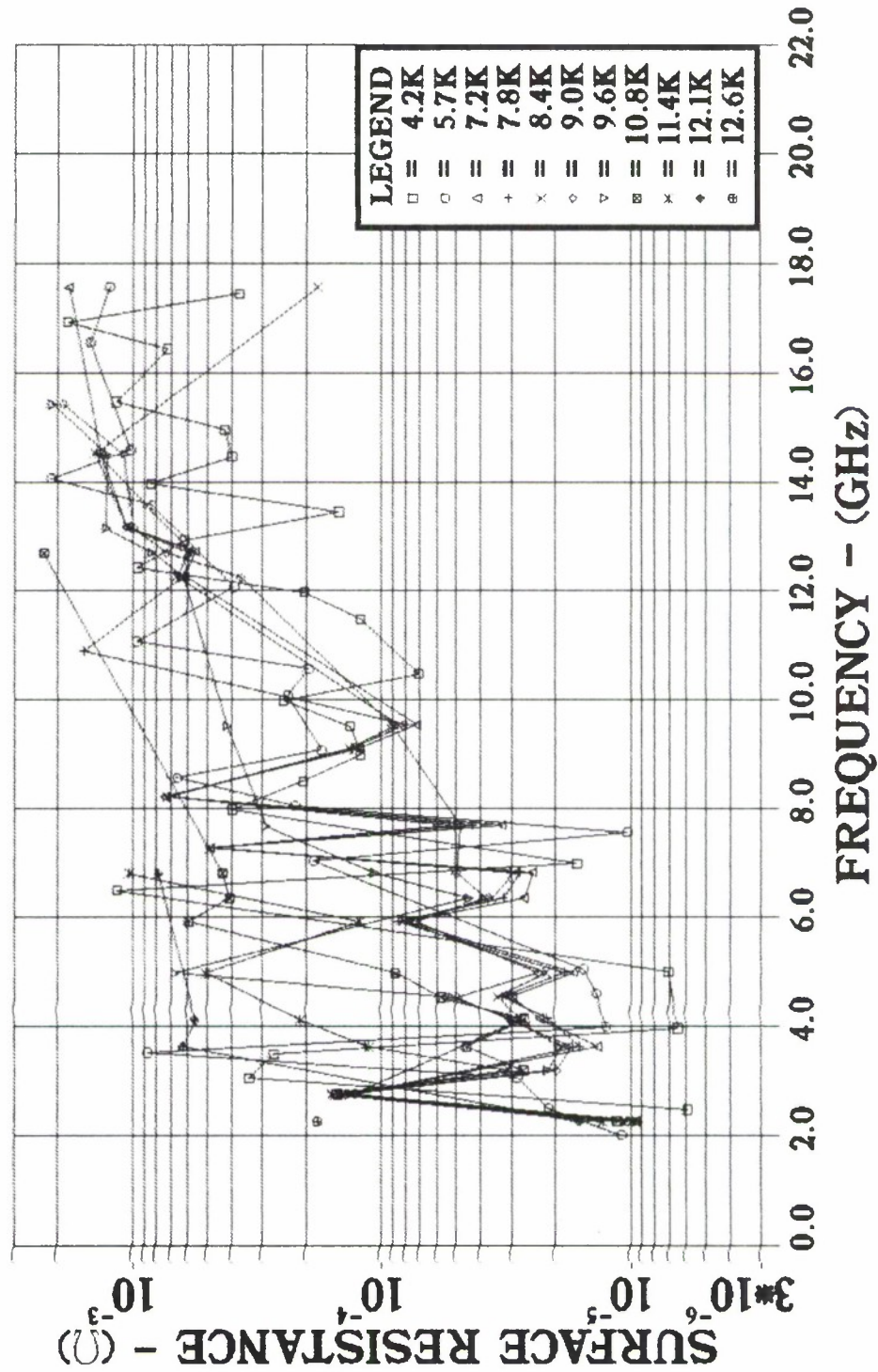


Figure 5. Variation of surface resistance with frequency for 1.5μm NbN film deposited on sapphire by reactive sputtering (600°C substrate). (Naval Research Laboratory)

Two important points should be noted. First, that the very small change of losses with temperature below 9 K indicates that losses in these films are still dominated by residual losses (See Appendix A). Second, that even these non-optimized films indicate that for devices operating up to 4 GHz this material can support TB products of more than 1000 for temperatures up to 12 K. This means that low loss delay lines can be operated in conjunction with commercially available closed-cycle cryocoolers.

2.3 Nb₃Sn Films

Films deposited by Laura Allen and William Anklam of the Ginzton Laboratory at Stanford University were evaluated. A typical result is shown in Fig. 6. Large variations of R_s with frequency are evident indicating possible inhomogenities in the film. One of the substrates that was used for the measurement of all the Stanford samples appears to be partially going to the normal state around 9 - 10 K. Substitution of this film by a niobium nitride film in the resonator indicates lower losses above 9 K but the large variations of Q with frequency still persist.

We have also evaluated films deposited by the group of Professor Nordman at the University of Wisconsin, Madison. These films were deposited by sequential sputtering followed by high temperature annealing. They were very lossy, with Q less than 1000 at 600 MHz and dropping below 100 at 1800 MHz. Measurements above 2 GHz could not be performed.

2.4 Discussion

Except for variations of the stripline coupling gap, the structures used to get the results for the Nb films deposited at Lincoln Laboratory and Nb and NbN films deposited elsewhere are exactly the same. The most striking difference is that while the results for films deposited at Lincoln Laboratory are smooth, films deposited everywhere have surface resistances that vary wildly with

Nb₃Sn - (STANFORD-I)

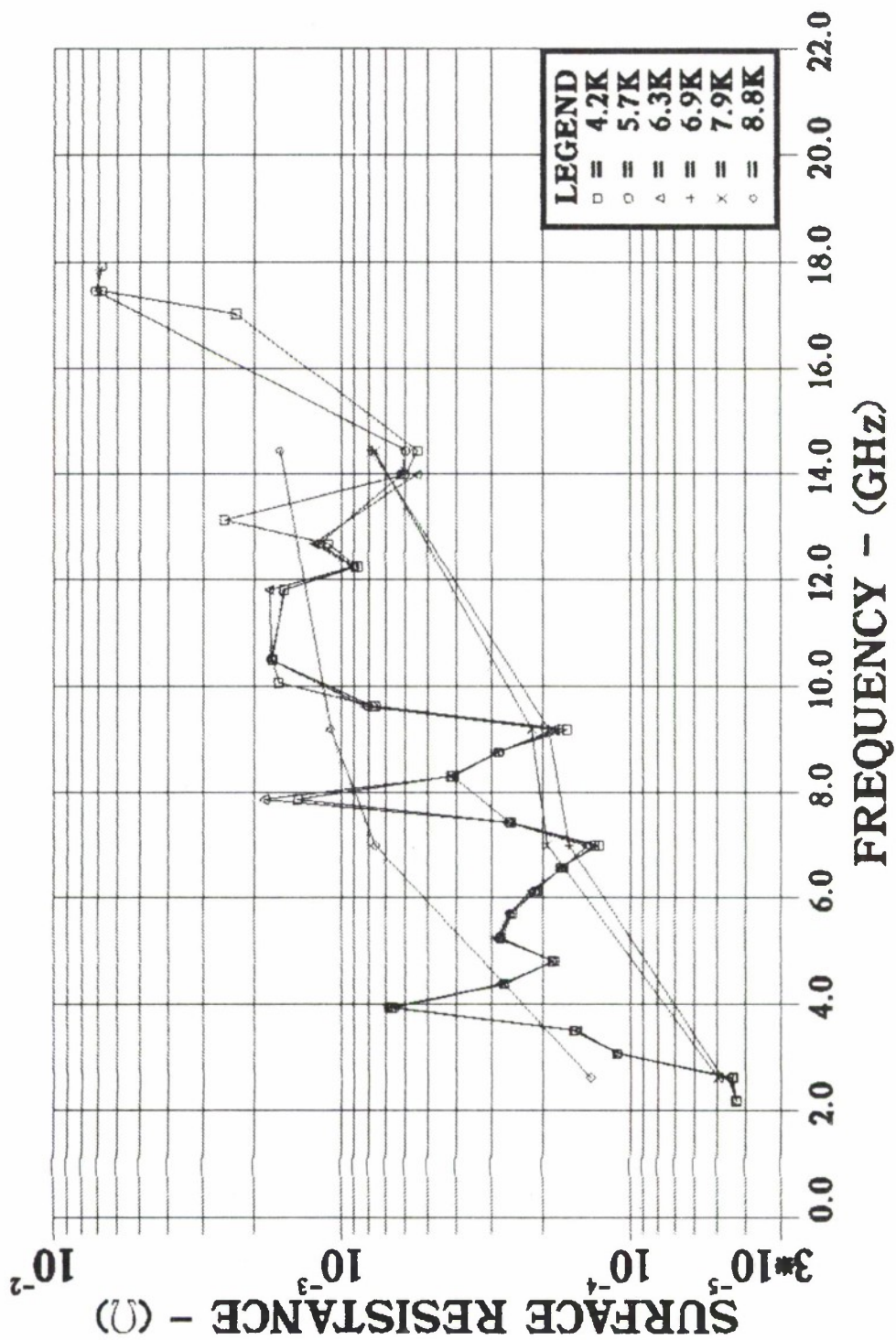


Figure 6. Variation of the surface resistance with frequency for Nb₃Sn film deposited on sapphire at the Ginzton Laboratory (Stanford University) by co-evaporation.

frequency. We believe that those variations are due to localized defects in the samples. For the samples deposited in-house, special care was taken to avoid contaminating the samples with particulates. Not only are the samples deposited in a system located in a clean room, but other special precautions were taken to avoid particulate contaminants during pump down. Indeed, one of the main problems in the development of our technology to fabricate long delay lines was the presence of particulates during deposition of niobium. This contamination introduced local variations in the quality of the film that created undesirable reflections on the striplines.

For the resonator structure used, different modes have different current distributions. If a certain mode is associated with a large current in a region where the film has been locally contaminated by a particulate, this will result in a low Q measurement. This hypothesis is further strengthened by our observation that all the films received from other laboratories are obviously severely contaminated by particulates when observed with dark field illumination under an optical microscope.

Despite these limitations the results with Nb₃Sn and NbN are encouraging since, assuming that our hypothesis about particulate contamination is correct, these materials, when cleanly deposited, should support long delay when operating at temperatures (near 11 K) compatible with existing closed-cycle refrigerators. As part of another program an existing sputtering system is being modified to allow for the magnetron deposition of high quality clean NbN.

The variation of R_g with frequency for the films deposited elsewhere should allow us to locate the imperfections on the stripline. We intend to do so and then to analyze these suspected spots using Auger to evaluate the films for composition variations.

3. Ion Beam Deposition of Nb and NbN Thin Films

Films of Nb and NbN were deposited using the system shown in Fig. 7. The system consists of an Ion Tech ion source fitted with 7.5-cm-diameter sputtering grids, a water cooled Nb target (MRC marz grade) and a substrate heater, all within a vacuum chamber that is pumped by sorption pumps and a cryopump. The chamber is fitted with a Meissner coil to pump water vapor. The base pressure with the Meissner coil cold is less than 5×10^{-8} Torr. The total ion beam current at 1500 eV of accelerating voltage can be as large as 100 mA. The heater consists of an alumina block resistively heated by a tungsten meander line deposited directly on the block. The temperature of the block is measured by using a chromel alumel thermocouple inserted in a hole drilled parallel to the surface of the block. Temperatures up to 700°C can be reached easily using this heater. The temperature of the block as evaluated by an infrared viewscope is uniform within $\pm 10^\circ\text{C}$.

3.1 Nb Films

Niobium films deposited onto substrates heated to 600°C (block temperature) using an argon ion beam had T_c of 9.2 K and a very sharp transition (less than 100 mK). RF loss measurements of these films, however, indicated higher losses than for films deposited at room temperature by RF sputtering even though these films had lower T_c than the ion beam deposited films. To try to understand this apparent contradiction, and, as part of a systematic evaluation of these films, x-ray diffractometer, Auger and SIMS analysis were performed. The x-ray results showed sharper and more intense diffraction peaks as is expected from films deposited at a higher temperature (larger grain size). The SIMS analysis revealed the presence of some argon and also Cr, Ni and Fe roughly in the same proportions as expected in stainless steel. To determine the source of this contamination a series of silicon wafers coated with thin films of Nb

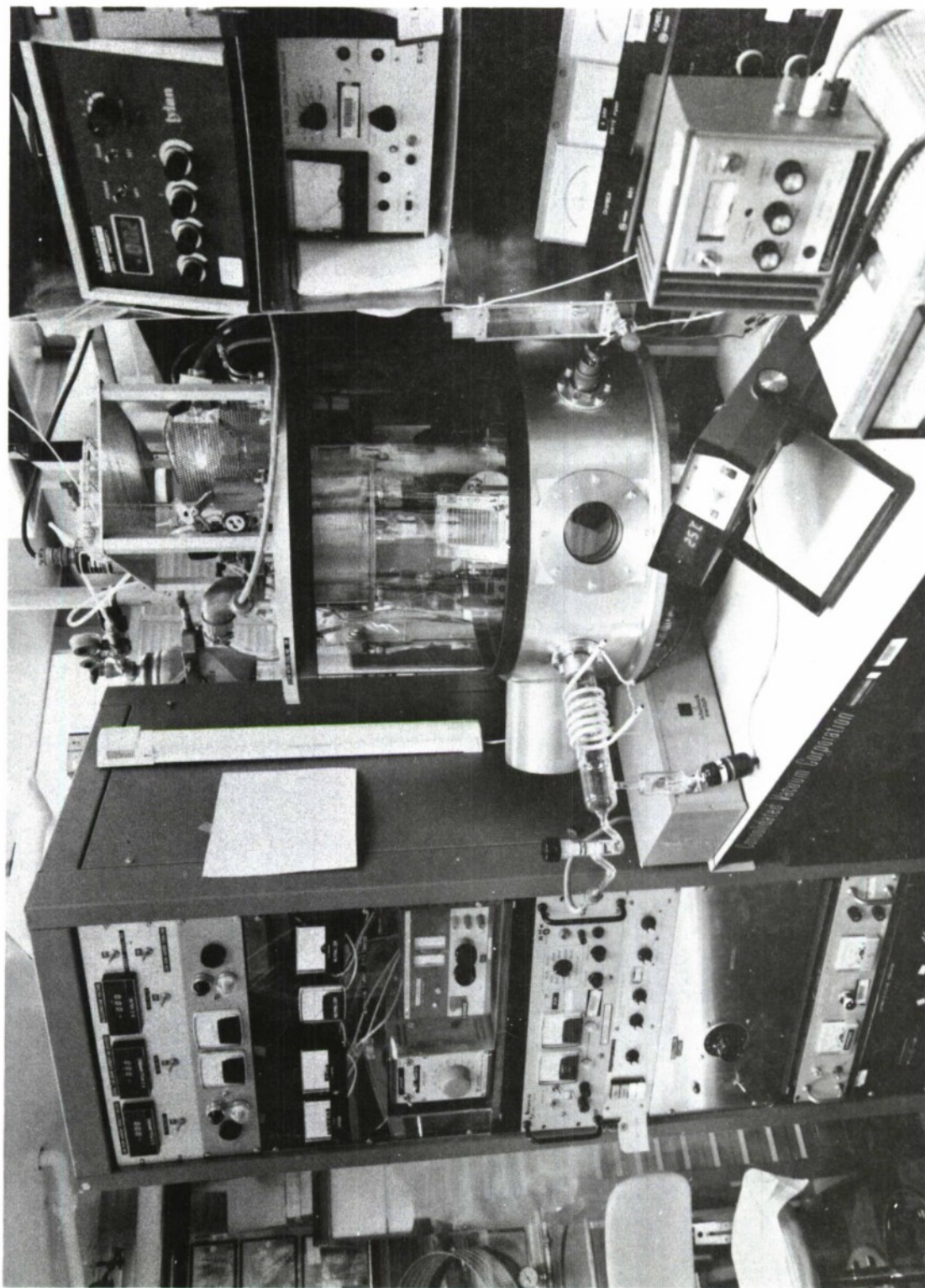


Figure 7. Ion beam deposition system.

and Cr were placed in different areas around the target. By evaluating the increase or decrease of the Nb or Cr thickness in these wafers we were able to determine what areas of the chamber were being bombarded by the ion beam. It was found that an area larger than the target was being bombarded even though the current density, as indicated by the etching rates of the Nb or Cr films, was very small outside of the target area. To improve upon this situation all the affected areas were covered with Nb foil and the beam collimation was enhanced using a Nb aperture as shown in Fig. 8. SIMS analysis in films deposited after these steps were taken indicated no Cr, Ni or Fe within the sensitivity of the instrument used (the instrument was not calibrated for a Nb matrix but we estimated the sensitivity to be better than 1 part/10000 based on some other samples purposely contaminated).

RF losses measurements for these films indicate losses slightly lower than for our sputtered films (but worse than for the films evaporated in UHV at 800°C).

3.2 NbN Films

NbN films were deposited by ion beam sputtering under the conditions indicated in Table I on both oxidized silicon (2200-Å thick SiO₂) and (0001) sapphire. The substrate holder was heated between 400°C and 675°C during deposition as shown in Table I. This was done since films deposited on heated substrates should have higher T_c and larger crystallite sizes. This should make it easier to maximize other parameters before attempting to deposit films at lower substrate temperatures. The films were patterned with a meander line using photolithographic techniques and reactive ion etching in CF₂Cl₂. The resistance of the patterned films (about 500 Sq) was then measured as a function of temperature. Representative results for these films are shown in Table I. The films were also evaluated using x-ray diffractometry and shown to be a

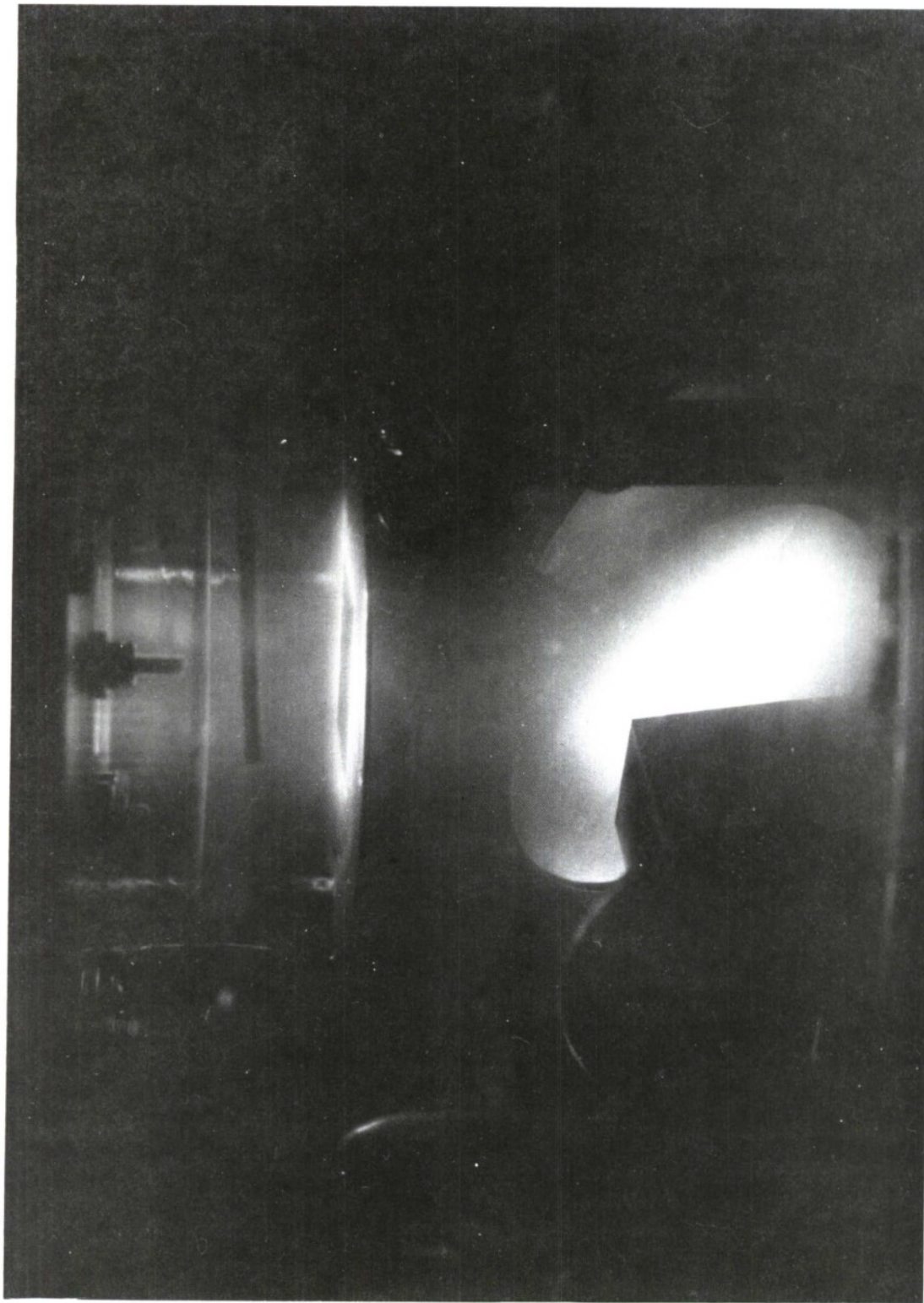


Figure 8. Detail of the chamber during deposition of a film showing the collimation of the ion-beam by Nb masks.

1189-85-1C

TABLE I

Deposition condition and properties of ion-beam-sputtered NbN thin films.

SAMPLE	SUBSTRATE	SUBSTRATE TEMPERATURE	ACCELERATION VOLTAGE	I _b CURRENT	DEPOSITION RATE	FILM THICKNESS	N ₂ PARTIAL PRESSURE	RRR 300K/20K	T _c K	ΔT _c K
Nb1b 142	n type S1 2200Å SiO ₂	425°C	1250V	75 mA	75Å/min	3500Å	1.3 x 10 ⁻⁴ Torr	.944	13.2	.25
Nb1b 143	n type S1 2200Å SiO ₂	425°C	1250V	75 mA	75Å/min	3400Å	1.3 x 10 ⁻⁴ Torr	.943	13.2	.28
Nb1b 144	(0001) sapphire	425°C	1250V	75 mA	75Å/min	3200Å	1.3 x 10 ⁻⁴ Torr	.92	13.8	.15
Nb1b 145	(0001) sapphire	445°C	1250V	75 mA	75Å/min	3200Å	1.3 x 10 ⁻⁴ Torr	.958	14.0	.10
Nb1b 146	(0001) sapphire	445°C	1250V	75 mA	75Å/min	3200Å	1.3 x 10 ⁻⁴ Torr	.911	13.9	.12
Nb1b 147	n type 2200Å SiO ₂	610°C	1250V	75 mA	75Å/min	3200Å	1.3 x 10 ⁻⁴ Torr	.908	13.9	.10
Nb1b 148	(0001) sapphire	525°C	1250V	75 mA	75Å/min	3200Å	1.3 x 10 ⁻⁴ Torr	.938	13.1	.18
Nb1b 150	(0001) sapphire	675°C	1250V	75 mA	75Å/min	2900Å	2.0 x 10 ⁻⁴ Torr	.998	11.2	.31

mixture of the hexagonal ϵ or δ' phase and of the δ NbN phase. Both (200) and (111) peaks of the δ phase were observed. Some very small and broad peaks may be associated with the β phase (Nb_2N).

The penetration depth for these films was evaluated using the GLAC theory in the dirt limit.² The results are indicated in Table II. The films were also evaluated using Auger spectroscopy. The atomic composition of the films was about 46% Nitrogen, 49% niobium and 5% oxygen. All the films evaluated to date were deposited with nitrogen introduced into the chamber and not into the ion source.

3.3 Discussion

The number of samples evaluated to date is small. The need to refurbish our facilities to allow for the construction of a clean room to lodge the new system that is presently being assembled (see below) limited the number of experiments that could be done in the old system. The results to date are at the same time encouraging and intriguing. We were able to obtain samples with relative high T_c (≈ 14 K) and fairly sharp transitions with ion beam deposition using N_2 introduced into the chamber. These results at first seem to contradict both the results of Jones et al³, who could only obtain superconductive films by ion beam deposition when N_2 was injected into the source, and those of Lin et al⁴, who could only obtain superconductive films when using a second ion source to bombard the film with N_2 ions. Jones et al, however, used a different type of ion source and Lin et al studied only films deposited at room temperature.

The very high resistivity of almost all samples deposited to date (see Table II) is another interesting point. The variation of resistivity with temperature for these samples is not very different from samples deposited elsewhere. We have not been able to evaluate crystallite size from the width of

TABLE II

Properties of ion-beam-sputtered NbN thin films.

SAMPLE	SUBSTRATE TEMPERATURE	RRR 300K/20K	RESISTIVITY	T _c	$\lambda(0)$
NbIb 142	425°C	.944	186- $\mu\Omega$ m	13.2 K	1.07Å
NbIb 145	610°C	.958	1820 $\mu\Omega$ m	14.0 K	1.03Å
NbIb 147	610°C	.908	910 $\mu\Omega$ m	13.9 K	7310Å
NbIb 148	525°C	.938	800 $\mu\Omega$ m	13.1 K	6890Å
NbIb 150	675°C	.998	46 $\mu\Omega$ /m	11.2 K	1840Å

the peaks in the x-ray diffraction measurements because of limitations with the x-ray equipment used. Better equipment is available and we intend to repeat the measurements in that equipment. However, comparison of the intensity of x-ray diffraction peaks with that of NRL samples indicate that we must have very small crystallites. A fractured sample does not show any structure when examined under SEM at 20000X. Sputtered and evaporated NbN are known to have a columnar structure and the low density regions between these columns, as well as O₂ segregation in these regions, could contribute to the observed high resistivity. The new system described in the next section, coupled with more careful structural analysis (including TEM cross sectional imaging) should allow us to further clarify this point.

3.4 The New Ion Beam System

It was our original intention as part of this contract to modify our ion beam deposition system with the use of an ion beam source capable of delivering a higher ion beam current (to increase the sputtering rate) and to add an additional setup to the chamber to create a local plasma in order to be able to vary the nitridation of the sample during the film deposition. These items are being incorporated in a new system.

Because of the large resistivity of the films deposited to date, which we think may be associated with the oxygen that is present in the films, we now feel that it was very important to reduce the partial pressure of oxygen and water during the film growth. Because of the relative low pressure in the chamber during the ion beam deposition, it is possible to use a partial pressure analyzer during the deposition of the films without any differential pumping. Partial pressures of water of 5×10^{-7} to 1×10^{-6} were measured during deposition despite the use of a liquid nitrogen cooled Meissner coil during the whole deposition process.

Accordingly, the manufacturers of the ion source and auxiliary ionizer (a Tri-Mag sputtering source) were approached with the purpose of modifying this equipment to allow for UHV compatibility. At the same time a new UHV chamber necessary for the installation of the new ion source and other equipment was designed and built. Provisions to bake the chamber to high temperatures (up to 400°C) and modifications to the cryopump to bring it to UHV specifications were also implemented. A picture of the new chamber with specially built support frame and lifter is shown in Fig. 9.

The system is now in its final stage of assembly.

4. Insulators

In order to have a complete high- T_c analog device technology both low loss conductors and low loss dielectrics are necessary.

For low loss transmission lines with appropriate impedances (20 Ω to 50 Ω) dielectric materials with thickness in the range 10 μm to 25 μm are necessary. These thicknesses are more in the realm of thick film than of thin film technology.

The chemical inertness of NbN suggests that it may be possible to use these films as ground planes upon which thick dielectric films can be deposited using thick film pastes.

During last summer we had occasion to experiment with some of these ideas with the help of a summer student (Lisa Maiocco). We selected eight different dielectric pastes from two different manufacturers. They were selected using as criteria low dielectric losses and good surface quality of the films.

To familiarize ourselves with the thick film technology and to determine the necessary parameters to form films of the right thickness and uniformity, a series of experiments using silicon wafers as substrates was performed. After

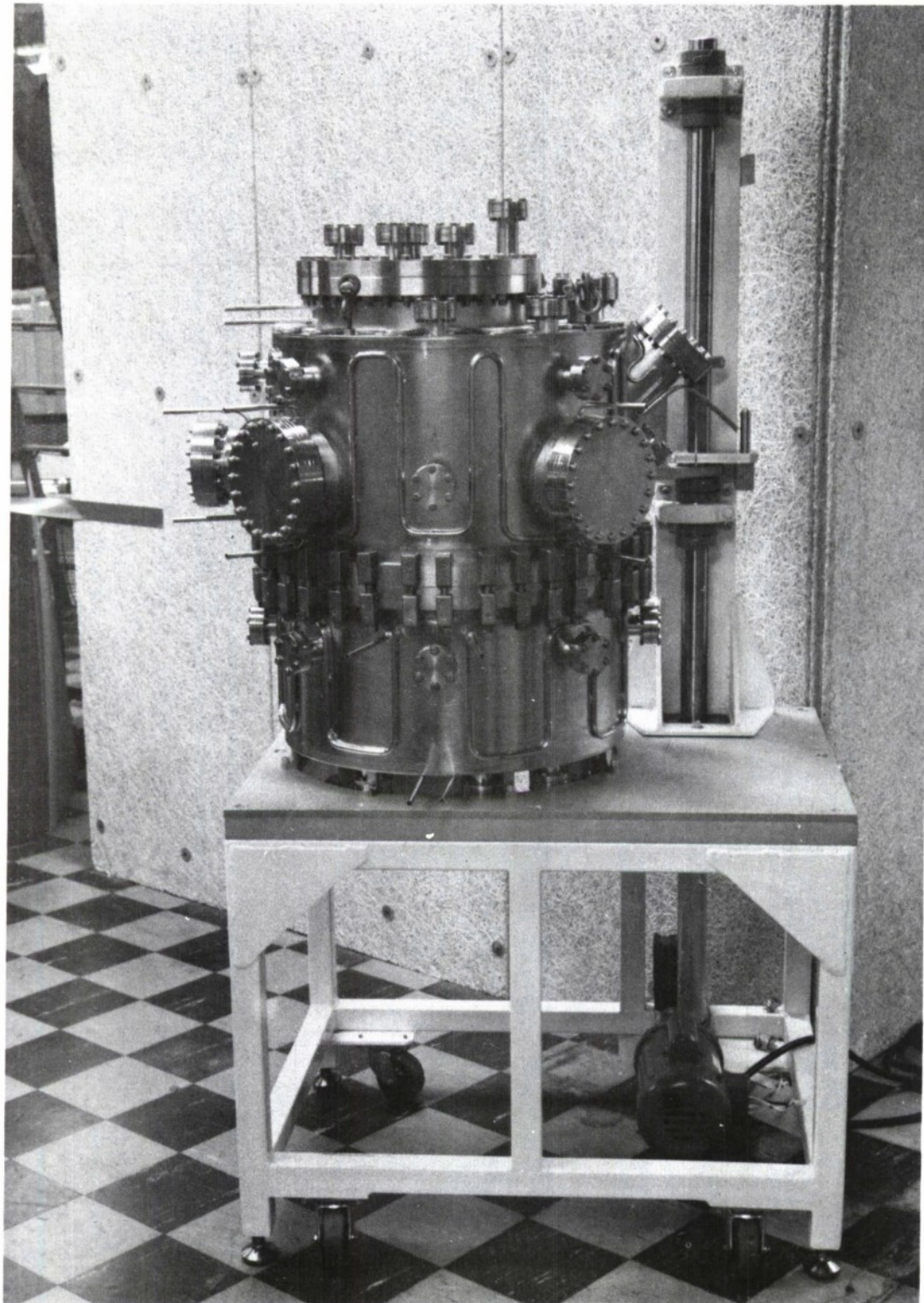


Figure 9. The new UHV chamber and support for the new ion beam deposition system.

these parameters had been determined, films were formed on silicon wafers on which a NbN film had been deposited by RF diode sputtering ($T_C \approx 14K$). Only two of the pastes adhered to the NbN well enough to allow for further evaluation. Preliminary results of an Auger analysis show that only a thin layer (about 100 Å) of the NbN reacted with the thick films. These two films are now being evaluated for dielectric losses.

5. Further Work

The new UHV system should become operational very soon. First, we will deposit films with parameters similar to the ones deposited in the old system to investigate the effect of the lower partial pressures of water and oxygen. The films will be evaluated using similar techniques as described before with special care being taken to characterize the uniformity of the films. The effect of the auxiliary nitrogen plasma will be then investigated systematically by varying the nitrogen pressure, plasma intensity (which can be varied by changing the electron beam current), ion energy (which can be adjusted by varying the RF or DC potential applied to the substrate), and substrate temperature.

For some representative films the penetration depth λ will also be measured using thin film delay line resonators. We intend to grow some NbN/Nb₂O₅/Pb alloy junctions using these films with methods similar to those we employ for the formation of Nb/Nb₂O₅/Pb-alloy junctions. This should allow us to approximately evaluate the gap parameter Δ for the NbN.

An effusion cell to allow for the evaporation of Sn in situ is being procured in order to form NbN/Nb₂O₅/Sn or NbN/insulator/Sn junctions. Because the system as presently configured represents an unique tool for the further investigation of a high- T_C technology, it is our intention to

extend this investigation to include the formation of junctions using artificial barriers. This investigation, however, is out of the scope of the present contract.

We will proceed with our investigation of the dielectric properties of thick films by using a capacitor structure at low frequencies (up to 13 MHz). If losses are respectable, we will then attempt to form films that are more uniform in thickness to allow for delay lines to be patterned. This will allow us to extend the dielectric losses measurements to the GHz range.

Our cooperation with other laboratories will continue. NbN films deposited at NRL, Westinghouse and Hypres and Nb₃Sn films deposited at Stanford and Westinghouse will be evaluated.

APPENDIX A

The voltage transfer function for the structure of Fig. 1 is ⁵

$$\frac{V_L}{V_S} = \frac{R_L}{R_L + 1/j\omega C_c} \left[2 \cosh \gamma \ell + \frac{Z_o}{R_L + 1/j\omega C_c} + \frac{R_L + 1/j\omega C_c}{Z_o} \sinh \gamma \ell \right]^{-1} \quad (A1)$$

where ω is the angular frequency, R_L the load and source resistance, Z_o the characteristic impedance of the stripline, C_c the coupling capacitance to the resonator, ℓ the resonator length, and $\gamma = \alpha + j\beta$ is the propagation constant of the stripline. The n th-order resonance implicit in Eqn. (A1) occurs for $\beta \ell \approx n\pi$, i.e., at frequencies $f_n = n v_p / 2\ell$ where v_p is the phase velocity of the line. The full-width at half-maximum of these resonances, Δf_n , determines the measured quality factor Q_{meas} .

$$Q_{\text{meas.}}^{-1} = \frac{\Delta f_n}{f_n} = Q_{\text{res}}^{-1} + Q_{\text{load}}^{-1} \quad (A2a)$$

Examination of Eqn (A1) near resonance shows that

$$Q_{\text{res}} = \frac{n\pi}{2\alpha\ell} \quad (A2b)$$

and

$$Q_{\text{load}} = n\pi / (4\omega^2 C_c^2 R_L Z_o) \quad (A2c)$$

The transmission insertion loss at the resonant peak is also given by Eqns. (A1) and (A2) and is

$$L = -20 \log_{10} \left| \frac{2V_L}{V_S} \right| = 20 \log_{10} \frac{(1 + Q_{\text{load}})}{Q_{\text{res}}} \quad (\text{A3})$$

The purpose of the measurement is the determination of the transmission line loss constant α . For this reason it is desirable that $Q_{\text{load}} \gg Q_{\text{res}}$ so that α may be inferred directly from Q_{meas} . Equation (A2) is used in design to select a coupling capacitance C_C small enough to guarantee this. From Eqn. (A3), it is evident that this light-loading condition is verified if the transmission loss at resonance exceeds 20 dB. On the other hand, if C_C is made too small, a large insertion loss results and measurements are made difficult.

Generally, the loss constant α is the sum of the conductor loss

$$\alpha_c = R/2Z_o, \quad (\text{A4a})$$

where R is the transmission-line series resistance per unit length, and the dielectric loss

$$\alpha_d = \omega \tan \delta / 2v_p \quad (\text{A4b})$$

where $\tan \delta$ is the loss tangent of the dielectric. In our measurements, the resonator geometry and dielectric loss tangents are such that the conductor losses dominate except at the lowest frequencies and temperatures.

Below their transition temperature T_C , superconductors have zero DC resistance. However, for alternating currents even a perfect superconductor will dissipate power. This occurs because, at non zero temperatures, not all electrons are in a superconductive state. The inertia of the superconductive electrons is manifested by a kinetic inductance and this, at non zero frequencies, leads to a voltage which drives the "normal" electrons which, in turn, transfer their energy to the lattice of the metal.

The temperature and frequency dependence of the surface resistance of a superconductor can be evaluated using the BCS weak-coupling theory.⁶ The general dependence cannot be obtained in a closed form but for $T < T_c/2$ the following approximation has been found to be accurate.⁷

$$R_s = R_o (f/f_o)^{1.7} \exp \left(- \frac{\Delta_o T_c}{T} \right) \quad (A5)$$

in which f_o and R_o are constants and Δ_o is the reduced energy gap. In practice, an additive temperature-independent term R_{res} has to be added to expression (A5) to account for other residual losses not covered by the Mattis-BCS theory.⁶ R_{res} , in general, will be very dependent on the deposition conditions of the superconductor.

For a stripline configuration R_s can be related to the attenuation constant of the transmission line by using a method developed by Wheeler.⁸ According to this method

$$\alpha_c = \frac{R_s}{Z_o} \sqrt{\frac{\epsilon}{\mu_o}} \left(\frac{\delta Z_o}{\delta b} - \frac{\delta Z_o}{\delta w} - \frac{\delta Z_o}{\delta t} \right) \quad (A6)$$

where b is the distance between the ground planes, t is the thickness of the conductor, w is the width of the conductor, and ϵ is the permittivity of the substrate.

Z_o can be calculated using any of many approximations. Expressions (A2b), (A3) and (A5) show that if $\alpha_c \gg \alpha_d$, $Q = f^{-0.7}$ and $L = \log(f^{-0.3})$. This dependence of Q and R_s on frequency is observed in some of our measurements which shows that in most cases we can ignore substrate losses for the frequencies of interest.

References

1. A. C. Anderson, R. S. Withers, S. A. Reible and R. W. Ralston "Substrates for Superconductive Analog Signal Processing Devices," IEEE Trans. Magn. MAG-19, pp. 485-489, (1983).
2. T. P. Orlando, E. J. McNiff, Jr., S. Foner and M. R. Beasley, "Critical Fields, Pauli paramagnetism limiting, and material parameters of Nb_3Sn and V_3Si ," Phys. Rev. B 19, PR 4545-4561, (1979).
3. H. Jones, J. Fischer and G. Bongi, "Some Superconducting and Normal State Properties of Niobium Nitride Thin Films," Solid State Commun. 14, pp. 1061-1064, (1974).
4. L. J. Lin, E. K. Track, G. J. Cui and D. E. Prober, "New Fabrication Technique and Electronic Tunneling Studies of NbN," to be published in Physica B.
5. R. L. Kautz, "Attenuation in Superconducting Striplines," IEEE Trans. Magn. MAG-15 (1979).
6. D. C. Mattis and J. Bardeen, "Theory of the Anomalous Skin Effect in Normal and Superconducting Metals," Phys. Rev. 111, pp. 412-417, (1958).
7. S. R. Stein and J. P. Turneaure, "Superconductive Resonators: High Stability Oscillators and Applications to Fundamental Physics and Metrology," in AIP Conference Proceedings, No. 44, (American Institute of Physics, New York, 1978), pp. 219-222.
8. H. A. Wheeler, "Formulas for the Skin Effect," Proceedings IRE 30, pp. 412-424, (1942).

UNCLASSIFIED

SECURITY CLASSIFICATION OF THIS PAGE (When Data Entered)

REPORT DOCUMENTATION PAGE		READ INSTRUCTIONS BEFORE COMPLETING FORM
1. REPORT NUMBER ESD-TR-85-317	2. GOVT ACCESSION NO.	3. RECIPIENT'S CATALOG NUMBER
4. TITLE (and Subtitle) Low-RF-Loss Superconductive Thin Film Alloys		5. TYPE OF REPORT & PERIOD COVERED Annual Report 1 June 1984 — 31 May 1985
		6. PERFORMING ORG. REPORT NUMBER None
7. AUTHOR(s) R.W. Ralston		8. CONTRACT OR GRANT NUMBER(s) F19628-85-C-0002
9. PERFORMING ORGANIZATION NAME AND ADDRESS Massachusetts Institute of Technology Lincoln Laboratory, P.O. Box 73 Lexington, MA 02173-0073		10. PROGRAM ELEMENT, PROJECT, TASK AREA & WORK UNIT NUMBERS
11. CONTROLLING OFFICE NAME AND ADDRESS Office of Naval Research 800 North Quincy Street Arlington VA 22217		12. REPORT DATE 31 May 1985
		13. NUMBER OF PAGES 38
14. MONITORING AGENCY NAME & ADDRESS (if different from Controlling Office) Electronic Systems Division Hanscom AFB, MA 01731		15. SECURITY CLASS. (of this Report) Unclassified
		15a. DECLASSIFICATION DOWNGRADING SCHEDULE
16. DISTRIBUTION STATEMENT (of this Report) Approved for public release; distribution unlimited.		
17. DISTRIBUTION STATEMENT (of the abstract entered in Block 20, if different from Report)		
18. SUPPLEMENTARY NOTES		
19. KEY WORDS (Continue on reverse side if necessary and identify by block number)		
<div style="display: flex; justify-content: space-between;"> <div> stripline resonators RF losses closed-cycle cryocoolers </div> <div> automated RF setup delay lines Nb shadow masks </div> </div>		
20. ABSTRACT (Continue on reverse side if necessary and identify by block number)		
<p>Stripline resonators in conjunction with an automated RF setup were used to determine RF losses in films of Nb, NbN and Nb₃Sn. Variation in the losses with frequency for some of these films seems to be associated with particulate contamination during deposition. However, measurements also indicate that if clean films can be deposited they could be used for very long delay lines (hundreds of nanoseconds) at temperatures compatible with existing closed-cycle cryocoolers.</p> <p>High RF losses in Nb films deposited by ion beam sputtering have been shown to be associated with contamination from stainless steel sputtered from fixtures in the chamber. Nb shadow masks were used to collimate the beam and this eliminated the problem. Reactively sputtered films of NbN deposited in this system onto heated substrates have transition temperatures as high as 14 K.</p> <p>A series of thick film pastes selected for their good insulating properties were used to form insulating layers on NbN. Two of these pastes adhered well to the NbN. Interaction with the NbN seems to be confined to a layer of 100 Å.</p>		